Bone Reports 11 (2019) 100213

Contents lists available at ScienceDirect

Bone Reports

journal homepage: www.elsevier.com/locate/bonr

MRI-derived bone porosity index correlates to bone composition and mechanical stiffness

Abigail L. Hong[a], Mikayel Ispiryan[a], Mugdha V. Padalkar[b], Brandon C. Jones[a,c], Alexandra S. Batzdorf[a], Snehal S. Shetye[c], Nancy Pleshko[b], Chamith S. Rajapakse[a,c,*]

[a] Department of Radiology, University of Pennsylvania, United States of America
[b] Department of Bioengineering, Temple University, United States of America
[c] Department of Orthopaedic Surgery, University of Pennsylvania, United States of America

ARTICLE INFO

Keywords:
MRI
Porosity index
Bone stiffness
Near infrared spectral imaging
Bone biomechanics
Magnetic resonance imaging
Ultrashort echo time

ABSTRACT

The MRI-derived porosity index (PI) is a non-invasively obtained biomarker based on an ultrashort echo time sequence that images both bound and pore water protons in bone, corresponding to water bound to organic collagenous matrix and freely moving water, respectively. This measure is known to strongly correlate with the actual volumetric cortical bone porosity. However, it is unknown whether PI may also be able to directly quantify bone organic composition and/or mechanical properties. We investigated this in human cadaveric tibiae by comparing PI values to near infrared spectral imaging (NIRSI) compositional data and mechanical compression data. Data were obtained from a cohort of eighteen tibiae from male and female donors with a mean ± SD age of 70 ± 21 years. Biomechanical stiffness in compression and NIRSI-derived collagen and bound water content all had significant inverse correlations with PI ($r = -0.79$, -0.73, and -0.95 and $p = 0.002$, 0.007, and < 0.001, respectively). The MRI-derived bone PI alone was a moderate predictor of bone stiffness ($R^2 = 0.63$, $p = 0.002$), and multivariate analyses showed that neither cortical bone cross-sectional area nor NIRSI values improved bone stiffness prediction compared to PI alone. However, NIRSI-obtained collagen and water data together were a moderate predictor of bone stiffness ($R^2 = 0.52$, $p = 0.04$). Our data validates the MRI-derived porosity index as a strong predictor of organic composition of bone and a moderate predictor of bone stiffness, and also provides preliminary evidence that NIRSI measures may be useful in future pre-clinical studies on bone pathology.

1. Introduction

Bone fractures pose a high risk to the aging and diseased population, and assessments of bone mineral density (BMD) are typically used to identify a patient's risk of fracture. For example, numerous studies have shown that women with low bone density in the radius or calcaneus are at increased risk of hip fracture (Gardsell et al., 1989; Hui et al., 1989; Cummings et al., 1990). Even with recent improvements in dual energy X-ray absorptiometry (DXA) and peripheral quantitative computed tomography (pQCT) (Sartoris and Resnick, 1989; Mazess et al., 1990; Maricic, 2014; Siu et al., 2003; Jamal et al., 2006; Sornay-Rendu et al., 2017), BMD has been demonstrated to only partially account for variability in bone quality (Bjornerem, 2016). Other factors, such as changes in bone's composition of collagen and water, have also been shown to contribute to bone strength (Keen et al., 1999; Viguet-Carrin et al., 2006; Wang et al., 2001; Li et al., 2014; Nyman et al., 2006).

Magnetic resonance imaging (MRI) ultrashort echo time (UTE) is an image acquisition protocol that has demonstrated considerable capability for imaging bone (Rajapakse et al., 2015; Horch et al., 2010; Manhard et al., 2016; Wurnig et al., 2014). UTE-MRI allows for direct imaging of bound and pore water in bone by acquiring signal with very short echo times (TE), on the order of 50 μsec, whereas conventional MRI cannot image bound water because the transverse relaxation time is too short (Rajapakse et al., 2015). UTE MR imaging of bone has been validated *via* comparison to μCT, pore water fraction, material composition, and mechanical testing, among others (Rajapakse et al., 2015; Bae et al., 2012; Chang et al., 2017a). Porosity index (PI) measurement is a recently introduced UTE-based methodology that has been successfully utilized to assess bone porosity *in vivo* in clinically practical acquisition times (Rajapakse et al., 2015). PI is obtained by measuring the signal decay in a single three-dimensional UTE examination that acquires signal at two echo times, 50 and 2000 μsec. The ratio of the

* Corresponding author at: Department of Radiology, University of Pennsylvania, United States of America.
E-mail address: chamith@mail.med.upenn.edu (C.S. Rajapakse).

https://doi.org/10.1016/j.bonr.2019.100213
Received 1 February 2019; Received in revised form 13 June 2019; Accepted 19 June 2019
Available online 26 June 2019

two signals allows for direct quantification of the water that is bound to collagen through hydrogen bonds in bone. This methodology overcomes the typical issue of limited resolution *in vivo* in purely structural imaging modalities (Al Mukaddam et al., 2014; Ahmed et al., 2015). Bone PI is strongly correlated with other measurements from bone structural imaging methods, including porosity obtained from micro computed tomography (μCT), bone density measured by pQCT, and pore water fraction measured using multi-echo UTE sequences (Rajapakse et al., 2015). Most notably, cortical bone PI was shown to strongly agree with μCT-evaluated cortical bone porosity fraction (R^2 = 0.79) (Rajapakse et al., 2015). The fact that PI can simultaneously image protons in both free water (pore water) and water bound to collagenous matrix (bound water) suggests that PI could also provide *in vivo* quantification of bone health by measuring both the amount and distribution of the organic components in bone, but it has not yet been validated compared to material composition imaging modalities or to mechanical testing. PI has the potential for clinical use to assess changes in cortical bone porosity that result from disease and in response to therapy, but additional work is needed to fully understand its usefulness.

Near-infrared spectral imaging (NIRSI) is a fast spectroscopic modality that effectively evaluates the spatial distribution of water and organic components in the imaged sample (Chang et al., 2017a). NIRSI measures signals from molecular vibrations resulting from incident radiation on the sample and is particularly adept at imaging organic components of human bone that contribute to variability in porosity and bone fragility, including water, collagen, and fat content. NIRSI, in contrast to more traditional methods of chemical analyses, evaluates intact samples non-destructively and requires limited or no sample preparation, with no chemical reagents and no waste production (Rajapakse et al., 2017a; Givens et al., 1997). Moreover, NIRSI images at higher frequencies than other mid-infrared imaging methods, allowing for greater penetration of the tissue, on the order of millimeters to centimeters (Rajapakse et al., 2017a). A recent study demonstrated that NIRSI-derived bone organic compositional parameters yielded remarkable agreement with bone UTE data (Chang et al., 2017a). A strong correlation was reported between the intensity of the two NIRSI water peaks and UTE-MRI bound water values (r = 0.74, 0.71). The minimal sample preparation, non-destructive nature of the scan, and relative speed of NIRSI makes it an ideal method for investigation of changes in water content, distribution, and environment in pre-clinical studies of bone pathology and therapeutics.

Here, we hypothesize that cortical PI can provide accurate measurements of bone organic material composition compared to NIRSI data. We further hypothesize that, due to its known ability to image structural data of bone, PI will provide accurate predictions of bone strength. As a secondary aim, we hypothesize that bone strength predictions will be further improved when PI is combined with direct quantification of material data from near-infrared spectral imaging. Our goals were two-fold: (1) assess correlations with PI, NIRSI, and biomechanical data, and (2) determine if PI, NIRSI, or a combination of the two would be effective at predicting mechanical stiffness as a measure of bone strength.

2. Materials and methods

2.1. Bone specimens

Eighteen fresh whole human cadaveric tibiae were harvested from six male (age 70 ± 17, range 49–83) and twelve female (age 65 ± 23, range 27–97) donors with no history of skeletal disease (NDRI, Philadelphia, PA). They were stored frozen at -30 °C and thawed for 6 h before imaging. Segments of whole tibiae 36-mm in length were cross-sectioned from the diaphysis at a distance approximately 38% proximal to distal endplate using a Hall Pneumatic reciprocating saw (Linvatec 11,311 Concept Blvd Largo, FL) for UTE-MRI imaging. From these segments, 450 μm thick whole cross-section samples were cut using a diamond wafering saw (Buehler Isomet 1000, Lake Bluff, IL) for NIR spectral imaging. All sectioned specimens were stored in a phosphate-buffered saline (PBS) solution (pH 7.4, Invitrogen, Carlsbad, CA) for at least one to two days at 4 °C before data collection. Of the eighteen tibiae used in this study, we were only able to perform all three tests of near infrared spectral imaging, PI, and mechanical testing on 9 of the samples, for reasons that are detailed in each respective section. Of the remaining 9 samples, 3 were tested with NIRSI and PI, 3 were mechanically tested and scanned for PI, and 3 were mechanically tested and analyzed with NIRSI.

2.2. Assessment of porosity index

Scanning was performed on a 3-T whole body MRI machine (Siemens Prisma, Erlangen, Germany) with a four-channel surface coil (Insight MR Imaging, Worcester, MA). The 36-mm thick bone specimen was scanned with the following parameters: field of view, 160 × 160 × 160 mm^3; repetition time, 12 msec; flip angle, 12° with 20 μsec hard pulse duration; 50,000 half-projections distributed uniformly within a sphere (34); 190 readout points per projection; gradient ramp time, 240 μsec; and readout bandwidth, 125 kHz. Two UTE images were reconstructed using TE of 50 and 2000 μsec onto a 320 × 320 × 320 matrix corresponding to an isotropic 0.5 mm voxel size. PI is the ratio between a long TE (TE_{long}) and the shortest TE (TE_{short}) obtained by the UTE image intensities:

$$\text{Porosity Index}\,(\%) = \frac{TE_{long}\ \text{intensity}}{TE_{short}\ \text{intensity}} \times 100$$

Theoretically, TE_{short} captures the proton signal from all water within the sample and TE_{long} is primarily derived from the freely moving pore water. The signal in the bone region from TE_{short} therefore appears much brighter than that of TE_{long}, as is illustrated in Fig. 1. Images acquired at TE of 2000 μsec and 50 μsec were used for the long and short TE images, respectively. The boundary between the trabecular and cortical compartments was manually segmented to include only dense cortical bone by a trained laboratory technician, similar to previously established methods (Rajapakse et al., 2015). For this study, the average voxel PI value within the cortical compartment was considered as the overall porosity. Cortical bone cross-sectional area (CbA) was also calculated from segmented UTE scans to improve multivariate regression analyses, which are described below. Briefly, the cross-sectional area for each slice was calculated by multiplying the number of pixels within the region of interest by the in-plane resolution. The cross-sectional area used in the analysis was the average over the entire volume of interest. Of the eighteen total tibiae tested in this study, three were unable to be scanned since the MRI scanner was unavailable within a few days of the cadavers being stored.

2.3. NIR spectral imaging

The 450 μm thick bone samples underwent NIR spectral imaging using a Perkin Elmer Spotlight 400 imaging spectrometer (Shelton, CT). Before imaging, the surface sample water was dried with a Kimwipe. The sample was contained between a glass slide and glass coverslip to minimize water loss. Imaging was conducted with the following parameters: frequency range, 4000–7800 cm^{-1}; spectral resolution, 64 cm^{-1}; and pixel resolution, 50 μm. Total imaging time was 20 min for each sample. Two scans were run for each sample and averaged in order to improve the signal-to-noise ratio. NIR spectral images were analyzed using ISys 5.0 software (Malvern Instruments, Columbia, MD). Absorbances of interest were at 7008 cm^{-1} for water (corresponding to O—H bond), which was previously shown to be inversely related to donor age, and at 4608 cm^{-1} for collagen (corresponding to C—H bonds) (Chang et al., 2017a; Luck, 1974). Integrated areas under the

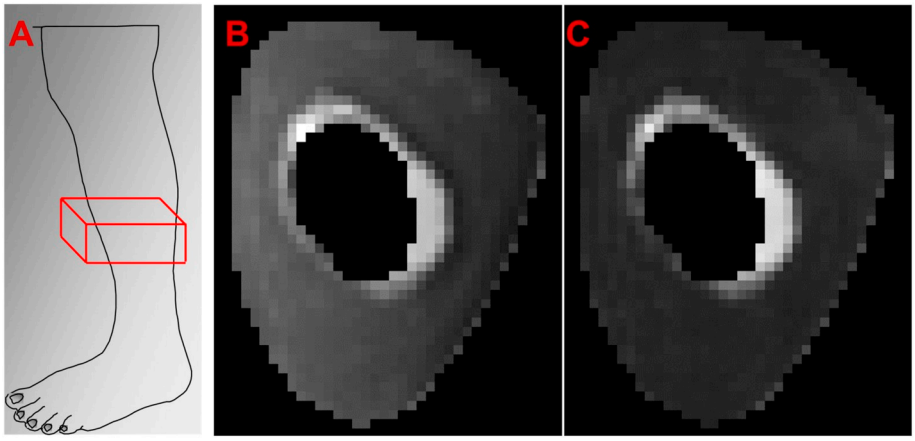

Fig. 1. A) Example location of mid-tibial scanning region for UTE scan. B) Representative image of TE_{short} from our UTE sequence. C) Representative image of TE_{long} from the same cadaver as in B, with a noticeably darker bone region than the corresponding TE_{short}.

NIRSI peaks were calculated to obtain water and collagen content as previously described (Chang et al., 2017a). Although spatially resolved data was collected at 50 μm resolution, the data were averaged across the bulk sample to maintain consistency with the parameters of the UTE-MRI data acquisition. It must be noted that three of the tibia samples were unusable for in-depth NIR spectral analysis because they were left in the PBS solution at 4 °C for over three days and thus water content was not considered reliable.

2.4. Biomechanical testing

Tibial segments 25 mm in length were obtained from the distal regions of the cadaver samples and then underwent uniaxial compression tests using a servo-hydraulic material testing machine (Instron 8874 Instron, Norwood, MA) equipped with a 100kN load cell. Each segment was loosely placed between two parallel steel plates and compressed according to a displacement rate of 1 mm/min until the ultimate load was reached. Whole-bone axial stiffness was found as the tangent of the initial linear portion of the force-displacement curve. Three of the cadaveric samples did not undergo mechanical testing due to unforeseen issues in sample preparation.

2.5. Statistical analysis

Statistical analyses were conducted using MATLAB (Mathworks, Natick, MA, USA), R (R Foundation for Statistical Computing, Vienna, Austria), and JMP Discovery Software (JMP 14.0; SAS Institute Inc., Cary, NC, USA) with $p < 0.05$ indicating statistical significance. Correlations between PI and other variables (stiffness, collagen, and bound water) were assessed using Pearson Correlation Coefficients (r) and p-values. PI was plotted against the other variables and displayed with a linear equation representing best fit and Pearson Correlation Coefficient (r). Next, multivariate regression analyses were conducted to evaluate the efficacy of the three imaging parameters (PI, collagen, and bound water) at predicting bone stiffness when combined into aggregate models. Separate regressions were run for each of our proposed models for predicting or stiffness. Comparisons were drawn between PI and NIRSI measurements to create a multi-faceted assessment of bone strength. For models that performed better than PI, ΔR^2 and p values were calculated to evaluate the usefulness of adding additional parameters. Partial R^2 tests were used to evaluate the significance of parameters at predicting bone stiffness when controlling for others.

3. Results

3.1. PI as a predictor of bone quality

Our results show strong negative correlations between PI and experimentally obtained bone stiffness ($r = -0.79$, $p = 0.002$), NIRSI determined collagen ($r = -0.73$, $p = 0.007$), and bound water content ($r = -0.95$, $p < 0.001$), respectively. Compositional and structural differences between old and young cadavers were clearly evident in NIRSI spectrum and PI values (see Fig. 2). Fig. 3 displays correlation graphs comparing PI with bone stiffness, collagen, and water content.

3.2. Multi-modality prediction of bone stiffness

Results of single and multivariate regression analyses for predictions of bone stiffness are listed in Table 1. PI exhibited moderate predictive efficacy for bone stiffness ($R^2 = 0.63$, $p = 0.002$). Cortical bone area also showed moderate predictive efficacy for bone stiffness ($R^2 = 0.40$, $p = 0.03$). The predictive accuracy of PI combined with CbA ($R^2 = 0.67$, $p = 0.01$) was better than that of CbA alone ($\Delta R^2 = 0.04$, $p = 0.48$) but not better than that of PI alone ($\Delta R^2 = 0.04$, $p = 0.48$).

Collagen alone and water alone did not predict bone stiffness ($R^2 = 0.01$, $p = 0.76$ and $R^2 = 0.12$, $p = 0.28$), but when both collagen and water were combined, the model was significant ($R^2 = 0.52$, $p = 0.04$). Furthermore, collagen controlling for water, and water controlling for collagen, each predicted stiffness (partial $R^2 = 0.46$, $p = 0.02$ and partial $R^2 = 0.52$, $p = 0.01$).

When collagen values were combined with MRI-derived PI ($R^2 = 0.72$, $p = 0.02$), the model was significant, but the predictive value did not increase compared to that of PI alone ($\Delta R^2 = 0.09$, $p = 0.21$). However, when either water or CbA was added to the PI and collagen model, the three-factor models did not predict stiffness. Water combined with PI also did not predict stiffness.

4. Discussion

The health and strength of bone is determined by numerous factors, including the quantity of mineralized tissue, the amount, distribution, and crosslinking ability of collagen, and the macro- and micro-structure of bone (Viguet-Carrin et al., 2006; Seeman and Delmas, 2006; Boskey, 2013). Bone's compressive strength comes from its high degree of mineralization, specifically hydroxyapatite, which constitutes approximately 60% of human bone (Seeman and Delmas, 2006). Total bone mineral content decreases with age, which is associated with increased fracture risk and decreased bone strength (Kanis, 2002; Leibson et al., 2002; Bolotin and Sievanen, 2001). The non-mineral component of

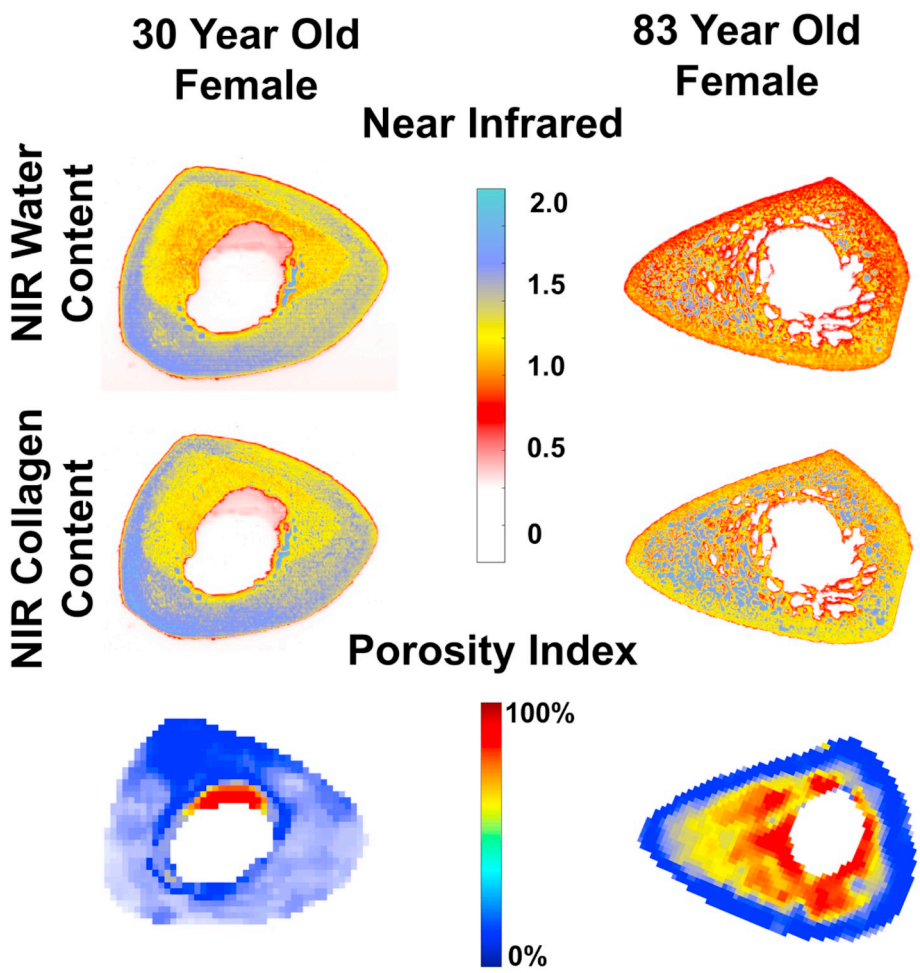

Fig. 2. Example of NIRSI collagen, water, and porosity index colormaps for two cadavers. The first column is a 30-year-old female and the second column is an 83-year-old female. Significant degradation of the endosteum can be seen in each scan of the older cadaver.

bone is an organic matrix mixture that is primarily comprised of collagen. Collagen provides bone with its tensile strength, in addition to stabilizing the extracellular matrix, supporting deposition of mineral crystals, and many other functions (Viguet-Carrin et al., 2006; Seeman and Delmas, 2006; Boskey, 2013). Analogously to the mineral content, bone collagen degrades with age, which causes a significant reduction in the toughness and health of bone (Wang et al., 2002). Research has shown that high bone stiffness is correlated to distribution of mineral as a continuous layer outside collagen fibrils compared to periodic distribution in staggered manner in collagen matrix (Abueidda et al., 2017). Moreover, studies have shown that age and osteoporosis are associated with an increase in the ratio of the mineral-to-matrix content and increased fracture risk (Gourion-Arsiquaud et al., 2009).

Concomitant to its material properties, the structural properties of bone have been shown to play an outsized role in the strength of bone. Morphological measures, including bone size and cross-sectional area, can predict up to 70% of bone strength and have outperformed BMD measurements in terms of fracture load prediction in certain bones (Augat and Schorlemmer, 2006). Additionally, the porosity of cortical bone has been shown to describe 65–80% of variations in Youngs moduli within the CbA (Currey, 1988; Dong and Guo, 2004).

Clinically, assessment of bone health is typically limited to mineralization measures in the form of BMD. Although BMD has proven to be a cheap and reliable measure of mineralization, it fails to account for the other factors determining bone strength, which limits its ability to accurately evaluate fracture risk (Bjornerem, 2016; Seeman and Delmas, 2006). Non-invasive and non-destructive methods of ascertaining the three-dimensional morphology and non-mineral composition of bone are therefore highly desirable to both clinicians and researchers.

MRI-UTE-derived PI is a recently introduced, clinically viable methodology that has been previously validated as a strong predictor of bone structural parameters (Rajapakse et al., 2015). This study further validated it as a useful non-invasive measure of the organic material compositions of bone. Cortical porosity index was significantly correlated with collagen and water content, with porosity index showing strong correlation with water and moderate correlation with collagen, respectively ($r = -0.73$ and $r = -0.95$). Moreover, our data showed that porosity index alone accounts for 63% of the variability in stiffness, making it a moderate predictor of bone strength. To further analyze the efficacy of PI, we performed a multivariate regression analysis with all imaging parameters obtained. While both PI alone and CbA alone predicted stiffness ($R^2 = 0.63$ and $R^2 = 0.40$), the ΔR^2 between the two-factor model and their individual regressions indicated that adding CbA did not improve the predictive accuracy of PI alone, while adding PI significantly improved upon CbA alone. This suggests that PI provides information related to stiffness that is not captured by CbA. Likewise, none of the remaining multivariate models predicted stiffness better than PI alone. It is not surprising that PI's relationship to bone strength is independent of cross-sectional area, since it is calculated as an average over the ROI and is therefore independent of scale or size. Additionally, the bone porosity is known to vary radially within the bone, increasing from the periosteum to the endosteum, and is independent of the total bone size (Rajapakse et al., 2015; Patsch et al.,

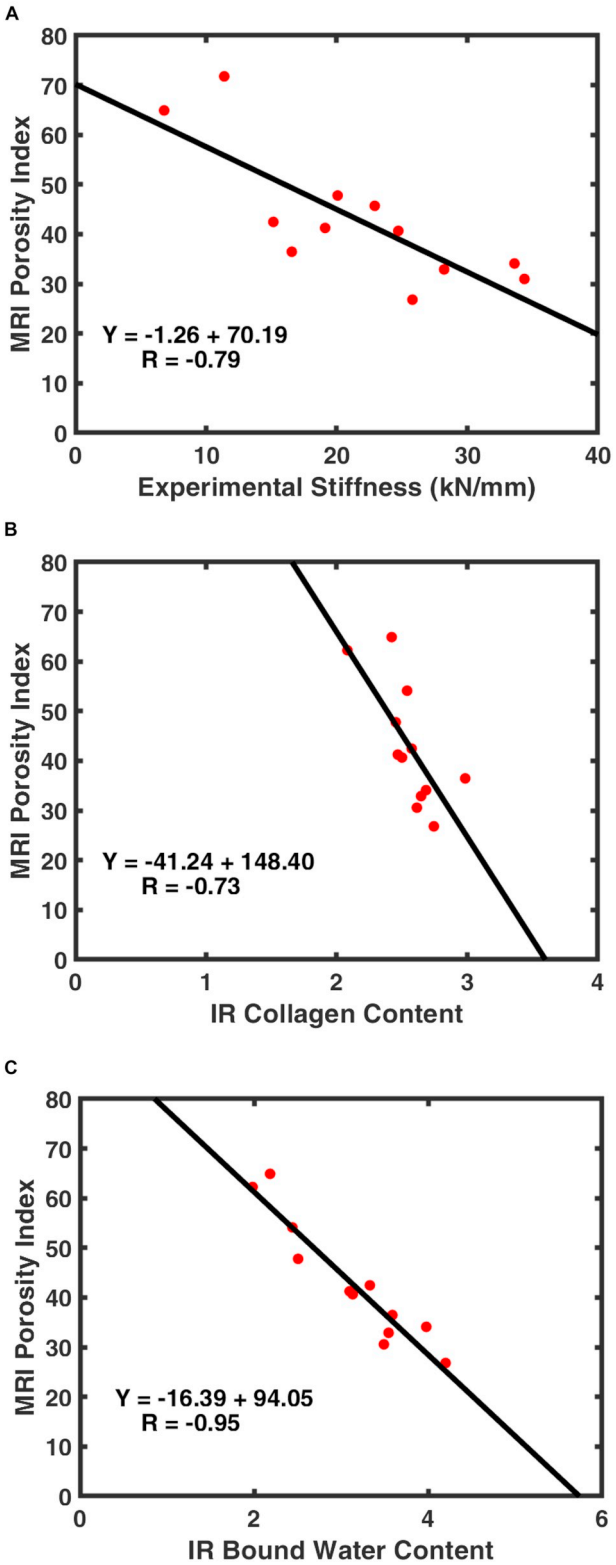

Fig. 3. Plotted correlations between MRI porosity index and A) experimentally obtained stiffness, B) NIRSI collagen content, and C) NIRSI water content.

2013). The data presented here suggest that porosity index is capable of measuring both structural properties and the organic composition of bone, as well as moderately predicting bone strength.

It is important to note that, while NIRSI collagen alone and NIRSI water alone did not correlate with bone stiffness, their combined model was significantly related to stiffness. Further analysis revealed that both values predict stiffness when you control for the other parameter, indicating that they are both related to bone strength, albeit in an indirect way. This makes sense since controlling for the other parameters helps to normalize the values with the overall size of the bone. Furthermore, this supports the notion that water and collagen are the two largest organic components in bone and the strength of bone is known to depend on its organic composition (Boskey, 2013). This further indicates that NIRSI could be useful in future pre-clinical studies investigating the effects of pathologies or pharmaceuticals on bone strength.

Table 1
Comparison of multivariate regression models predicting stiffness.

	N	R^2	p
PI	12	0.63	0.002*
Cortical area	12	0.40	0.03*
PI + cortical area	12	0.65	0.01*
Collagen	12	0.01	0.76
Water	12	0.12	0.28
Collagen + water	12	0.52	0.04*
PI + collagen	9	0.72	0.02*
PI + water	9	0.63	0.05
PI + collagen + water	9	0.72	0.07
PI + collagen + cortical area	9	0.74	0.06

Water makes up approximately 20% of the volume in cortical bone, so the volume of pore water located in the vascular-lacunar-canalicular space is strongly correlated with bone porosity. This value has been consistently reported; Biexponential analysis by Du et al. (Du et al., 2013) found the pore water fraction to be approximately 22% in the mid-tibia of human cortical bone, and the Carr-Purcell-Meiboom-Gill sequence analysis by Horch et al. (Horch et al., 2010) reported a similar 23% fraction in the mid-femoral cortex. Bound water is a significant factor in predicting the biomechanical properties of bone and is responsible for giving collagen its ability to confer ductility or plasticity to bone. Dehydration causes bones to become brittle, while also increasing stiffness and strength (Granke et al., 2015). Therefore, it is not surprising that PI was found to strongly predict bone strength.

PI has been applied to the assessment of bone quality in a study that investigated a cohort of 68 healthy men and women who underwent 3D UTE-MRI (3.0T) of both their femoral neck and tibia (Chen and Yuan, 2018). Chen et al. sought to draw scientifically and clinically important relationships between the obtained *in vivo* PI values and factors such as age and BMI. Femoral neck PI was found to be negatively correlated with age ($R^2 = 0.15$) and curvilinearly correlated with BMI ($R^2 = 0.23$) in men. Tibial PI was positively correlated with age ($R^2 = 0.22$) in postmenopausal women and negatively correlated with BMI ($R^2 = 0.23$) in all women. Additionally, femoral PI was significantly higher in men than in women ($p < 0.001$). Given the results of this study, Chen's findings make sense, since both collagen and bone structure are known to diminish with age (Viguet-Carrin et al., 2006; Seeman and Delmas, 2006; Boskey, 2013). However, it is important to note that there was no correlation between the femoral neck and tibial PI, so they cannot be used as substitutes for each other in assessing bone quality. Further studies will be needed to assess the variation of porosity indices in different bones within-subject, as well as to evaluate their ability to predict bone fracture.

In addition to measuring BMD, other less common clinical methods for assessing bone strength include 3D image-based assessment of bone structure and image-derived finite element models (Kopperdahl et al., 2014; Chang et al., 2017b). Of these, a commonly researched method in the past few decades is CT-derived finite element analysis (FEA), which combines bone structural information with measurements of BMD. Although this has shown good efficacy at predicting bone fractures, it produces ionizing radiation. Recently, MRI-based FEA, which incorporates *in vivo* microarchitecture of bone, has been used to simulate bone strength without radiation (Rajapakse et al., 2017b). However,

FEA based on ^{1}H MRI does not directly include bone compositional data and instead infers it from the magnitude of the intensities of the marrow and bone imaged. Since the data presented indicates that PI can quantify the organic composition of bone in the form of collagen and water, it is possible that PI could be used to improve clinical bone strength evaluation when combined with measures of bone mineral density or with image based finite element models.

This study does include some limitations that could be improved upon in future research. The ideal first TE for the porosity index measurements is as short as possible to minimize the decay of total bone water signal. However, our current instrumentation allowed a minimum TE of 50 μsec for the first echo. The signal loss at this time is approximately 1% for the free water component and approximately 14% for the bound water component. The 7008 cm^{-1} NIRSI absorbance arises due to differing origins and environments, including pore water, water loosely bound to mineral or collagen, water structurally incorporated into mineral or collagen, or a combination thereof. There could also be potential interference of non-water OH bonds such as P-OH, which can be found on the surface or within apatite crystals, making the association between IR measures and bone strength not straightforward (Kolmas et al., 2015). Another limitation of this study is how the boundary between the cortical and trabecular bone compartments was identified. More specifically, the boundary between the two was carefully manually segmented to only include dense cortical bone. In addition to the obvious potential for erroneous segmentation, the efficacy of PI at predicting bone strength is likely to be lower in older cadavers, since the cortical compartment is less susceptible to remodeling and endosteal absorption than the trabecular compartment and would thus represent a smaller fraction of the total bone strength in older specimens (Clarke, 2008).

Validation of the porosity index biomarker as a predictor of the mechanical stiffness of bone could provide clinicians with a simple, non-invasive tool for assessment of bone fracture risk. Insight into a patient's bone porosity and stiffness parameters allows for evaluative measures to take place in preventative care, risk management of critical bone fractures, and evaluation of treatment efficacy.

Transparency document

The Transparency document associated with this article can be found, in online version.

Acknowledgements

This study was supported by NIH R01 AR068382, NIH R01 AR066008, NIH R21 AR071704, NIH T32EB020087, and Penn Center for Musculoskeletal Disorders award number P30AR069619.

References

Abueidda, D.W., Sabet, F.A., Jasiuk, I.M., 2017. Modeling of stiffness and strength of bone at nanoscale. J. Biomech. Eng. 139 (5).
Ahmed, L.A., et al., 2015. Measurement of cortical porosity of the proximal femur improves identification of women with nonvertebral fragility fractures. Osteoporos. Int. 26 (8), 2137–2146.
Al Mukaddam, M., et al., 2014. Effects of testosterone and growth hormone on the structural and mechanical properties of bone by micro-MRI in the distal tibia of men with hypopituitarism. J. Clin. Endocrinol. Metab. 99 (4), 1236–1244.
Augat, P., Schorlemmer, S., 2006. The role of cortical bone and its microstructure in bone strength. Age Ageing 35 (Suppl. 2), ii27–ii31.
Bae, W.C., et al., 2012. Quantitative ultrashort echo time (UTE) MRI of human cortical bone: correlation with porosity and biomechanical properties. J. Bone Miner. Res. 27 (4), 848–857.
Bjornerem, A., 2016. The clinical contribution of cortical porosity to fragility fractures. Bonekey Rep 5, 846.
Bolotin, H.H., Sievanen, H., 2001. Inaccuracies inherent in dual-energy X-ray absorptiometry in vivo bone mineral density can seriously mislead diagnostic/prognostic interpretations of patient-specific bone fragility. J. Bone Miner. Res. 16 (5), 799–805.
Boskey, A.L., 2013. Bone composition: relationship to bone fragility and antiosteoporotic drug effects. Bonekey Rep 2, 447.
Chang, G., et al., 2017a. MRI assessment of bone structure and microarchitecture. JMRI 46 (2), 323.
Chang, G., et al., 2017b. MRI assessment of bone structure and microarchitecture. J. Magn. Reson. Imaging 46 (2), 323–337.
Chen, M., Yuan, H., 2018. Assessment of porosity index of the femoral neck and tibia by 3D ultra-short echo-time MRI. J. Magn. Reson. Imaging 47 (3), 820–828.
Clarke, B., 2008. Normal bone anatomy and physiology. Clinical journal of the American Society of Nephrology : CJASN 3 (Suppl. 3), S131–S139.
Cummings, S.R., Black, D.M., Nevitt, M.C., 1990. Appendicular bone density and age predict hip fracture in women. JAMA 263, 665–668.
Currey, J.D., 1988. The effect of porosity and mineral content on the Young's modulus of elasticity of compact bone. J. Biomech. 21 (2), 131–139.
Dong, X.N., Guo, X.E., 2004. The dependence of transversely isotropic elasticity of human femoral cortical bone on porosity. J. Biomech. 37 (8), 1281–1287.
Du, J., et al., 2013. Assessment of cortical bone with clinical and ultrashort echo time sequences. Magn. Reson. Med. 70 (3), 697–704.
Gardsell, P., Johnell, O., Nilsson, B.E., 1989. Predicting fractures in women by using forearm bone densitometry. Calcif. Tissue Int. 44, 235–242.
Givens, D.I., De Boever, J.L., Deaville, E.R., 1997. The principles, practices and some future applications of near infrared spectroscopy for predicting the nutritive value of foods for animals and humans. Nutr. Res. Rev. 10 (1), 83–114.
Gourion-Arsiquaud, S., et al., 2009. Use of FTIR spectroscopic imaging to identify parameters associated with fragility fracture. J. Bone Miner. Res. 24 (9), 1565–1571.
Granke, M., Does, M., Nyman, J., 2015. The role of water compartments in the material properties of cortical bone. Calcif. Tissue Int. 97 (3), 292–307.
Horch, R., et al., 2010. Characterization of 1H NMR signal in human cortical bone for magnetic resonance imaging. Magn. Reson. Med. 64 (3), 680–687.
Hui, S.L., Slemenda, C.W., Johnston, C.C., 1989. Baseline measurement of bone mass predicts fracture in white women. Ann. Intern. Med. 111, 355–361.
Jamal, S.A., et al., 2006. Cortical PQCT measures are associated with fractures in dialysis patients. J. Bone Miner. Res. 21 (4), 543–548.
Kanis, J.A., 2002. Diagnosis of osteoporosis and assessment of fracture risk. Lancet 359 (9321), 1929–1936.
Keen, R.W., et al., 1999. Association of polymorphism at the type I collagen (COL1A1) locus with reduced bone mineral density, increased fracture risk, and increased collagen turnover. Arthritis & Rheumatism 42 (2), 285–290.
Kolmas, J., Marek, D., Kolodziejski, W., 2015. Near-infrared (NIR) spectroscopy of synthetic hydroxyapatites and human dental tissues. Appl. Spectrosc. 69 (8), 902–912.
Kopperdahl, D.L., et al., 2014. Assessment of incident spine and hip fractures in women and men using finite element analysis of CT scans. J. Bone Miner. Res. 29 (3), 570–580.
Leibson, C.L., et al., 2002. Mortality, disability, and nursing home use for persons with and without hip fracture: a population-based study. J. Am. Geriatr. Soc. 50 (10), 1644–1650.
Li, C., et al., 2014. Cortical bone water concentration: dependence of MR imaging measures on age and pore volume fraction. Radiology 272 (3), 796–806.
Luck, W.A., 1974. Structure of Water and Aqueous Solutions. Verlag Chemie.
Manhard, M.K., et al., 2016. MRI-derived bound and pore water concentrations as predictors of fracture resistance. Bone 87, 1–10.
Maricic, M., 2014. Use of DXA-based technology for detection and assessment of risk of vertebral fracture in rheumatology practice. Curr. Rheumatol. Rep. 16, 435–436.
Mazess, R.B., et al., 1990. Dual-energy x-ray absorptiometry for total-body and regional bone-mineral and soft-tissue composition. Amer J of Clin Nutr 51 (6), 1106–1112.
Nyman, J.S., et al., 2006. The influence of water removal on the strength and toughness of cortical bone. J. Biomech. 39 (5), 931–938.
Patsch, J.M., et al., 2013. Increased cortical porosity in type 2 diabetic postmenopausal women with fragility fractures. J. Bone Miner. Res. 28 (2), 313–324.
Rajapakse, C.S., et al., 2015. Volumetric cortical bone porosity assessment with MR imaging: validation and clinical feasibility. Radiology 276 (2), 526.
Rajapakse, C.S., et al., 2017a. Non-destructive NIR spectral imaging assessment of bone water: comparison to MRI measurements. Bone 103, 116–124.
Rajapakse, C.S., et al., Accuracy of MRI-Based Finite Element Assessment of Distal Tibia Compared to Mechanical Testing, in Bone, S.K. Boyd, Editor. 2017b.
Sartoris, D.J., Resnick, D., 1989. Dual energy radiographic absorptiometry for bone densitometry: current status and perception. AJR 152, 241–246.
Seeman, E., Delmas, P.D., 2006. Bone quality–the material and structural basis of bone strength and fragility. N. Engl. J. Med. 354 (21), 2250–2261.
Siu, W.S., Qin, L., Leung, K.S., 2003. pQCT bone strength index may serve as a better predictor than bone mineral density for long bone breaking strength. J. Bone Miner. Metab. 21 (5), 316–322.
Sornay-Rendu, E., et al., 2017. Bone microarchitecture assessed by HR-pQCT as predictor of fracture risk in postmenopausal women: the OFELY study. J. Bone Miner. Res. 32 (6), 1243–1251.
Viguet-Carrin, S., Garnero, P., Delmas, P.D., 2006. The role of collagen in bone strength. Osteoporos. Int. 17 (3), 319–336.
Wang, X., et al., 2001. The role of collagen in determining bone mechanical properties. J. Orthop. Res. 19 (6), 1021–1026.
Wang, X., et al., 2002. Age-related changes in the collagen network and toughness of bone. Bone 31 (1), 1–7.
Wurnig, M.C., et al., 2014. Characterization of trabecular bone density with ultra-short echo-time MRI at 1.5, 3.0 and 7.0 T – comparison with micro-computed tomography. NMR Biomed. 27 (10), 1159–1166.